Accurate Computed Enthalpies of Spin Crossover in Iron and Cobalt Complexes

Kasper P. Jensen*,† and Jordi Cirera‡

Technical University of Denmark, Chemistry-DTU, Building 207, DK-2800 Kgs. Lyngby, Denmark, and Department of Chemistry, Stanford University, Stanford, California 94305-5080

Received: January 22, 2009; Revised Manuscript Received: July 9, 2009

Despite their importance in many chemical processes, the relative energies of spin states of transition metal complexes have so far been haunted by large computational errors. By the use of six functionals, B3LYP, BP86, TPSS, TPSSh, M06, and M06L, this work studies nine complexes (seven with iron and two with cobalt) for which experimental enthalpies of spin crossover are available. It is shown that such enthalpies can be used as quantitative benchmarks of a functional's ability to balance electron correlation in both the involved states. TPSSh achieves an unprecedented mean absolute error of ∼11 kJ/mol in spin transition energies, with the local functional M06L a distant second (25 kJ/mol). Other tested functionals give mean absolute errors of 40 kJ/mol or more. This work confirms earlier suggestions that 10% exact exchange is near-optimal for describing the electron correlation effects of first-row transition metal systems. Furthermore, it is shown that given an experimental structure of an iron complex, TPSSh can predict the electronic state corresponding to that experimental structure. We recommend this functional as current state-of-the-art for studying spin crossover and relative energies of close-lying electronic configurations in first-row transition metal systems.

Introduction

Density functional theory (DFT)[1,2] is currently the most widely used theoretical method for describing electronic structure because of the unparalleled combination of computational speed and accuracy.[3−5] From fundamental theory, it is known that the method can in principle describe any molecular system to any desired accuracy, but unfortunately, no universal functional exists that describes accurately the energy of any given electron density.[1] Thus, scientists rely on a variety of functionals with various strengths and weaknesses, depending on the systems and properties studied.

To better compare these strengths and weaknesses, functionals can be divided into several classes: (i) those that depend solely on the density (local spin density approximations); (ii) those that depend also on the gradient of the density (generalized gradient approximation, GGA); (iii) those that in addition depend on the kinetic energy density (meta functionals);[6] (iv) those that combine the exchange functional from one of the above classes with some amount of "exact" exchange from the determinant wave function into so-called hybrid functionals.[7] With these four ingredients, modern DFT possesses a rigorous foundation but also faces a large and complex task of optimization and calibration against experimental data.[8]

Historically, most density functionals, like other theoretical methods, have been developed with particular emphasis on main-group elements.[9] For many such systems, hybrid functionals have been found to perform very well for both structures and many types of chemical energies:[1] B3LYP with 20% exact exchange displays an impressive mean absolute error (MAE) of ca. 10 kJ/mol for atomization energies, 5 kJ/mol for proton affinities, and 0.14 eV for ionization potentials for main-group molecules in the "G2" test set.[7] This success has made B3LYP the currently most used functional, probably also within the field of transition metal chemistry.[10,11]

However, when moving from main-block elements to other parts of the periodic table, in particular to systems involving transition metals, problems arise, since electronic configurations come very close in energy and enhance nondynamical correlation.[12,13] Some properties can be modeled well almost regardless of functional, e.g., structures, vibration frequencies, and some energies of reactions where the electronic structure is qualitatively unaltered, i.e., the number and types of occupied orbitals remain the same during the process (isodesmic reactions such as simple isomerizations and conformational equilibria).[10,14] Nonhybrid GGA functionals such as BP86[15,16] have been seen to work better for many transition metal systems, including processes such as ligand-binding to metal centers,[3,12] homolytic cleavage,[17] one-electron transfer, and spin inversion.[18]

Processes where the electronic structure changes qualitatively, i.e., where the quantum numbers of occupied orbitals change, are very sensitive to the description of exchange (or Fermi) correlation, which makes up the major component of the correlation energy.[12,17,19] The exact exchange component of hybrid functionals leads to a bias toward higher quantum numbers[17,18,20,21] and to underestimated bond dissociation energies by favoring the dissociated state.[12,17] The involved errors are substantial: average errors in bond energies are ∼50 kJ/mol with largest errors of ∼100 kJ/mol, and the systematic error component is substantial.[12]

The optimal amount of exact exchange depends on the coupling between electrons in the system of study, as implied by the adiabatic connection formula.[22] Perturbation theory partly explains why 20−25% exact exchange, as seen in B3LYP and PBE0, performs well for main group elements, whereas near-degenerate ground states with more nondynamical correlation require less exact exchange.[23] Not just theoretical considerations, but also computations benchmarked against empirical data indicate that 0−20% exact exchange is optimal in first-row transition metal systems.[19,24,25] In particular, a recent systematic

* To whom correspondence should be addressed. E-mail: kpj@kemi.dtu.dk.
† Technical University of Denmark.
‡ Stanford University.

10.1021/jp900654j CCC: $40.75 © 2009 American Chemical Society
Published on Web 08/21/2009

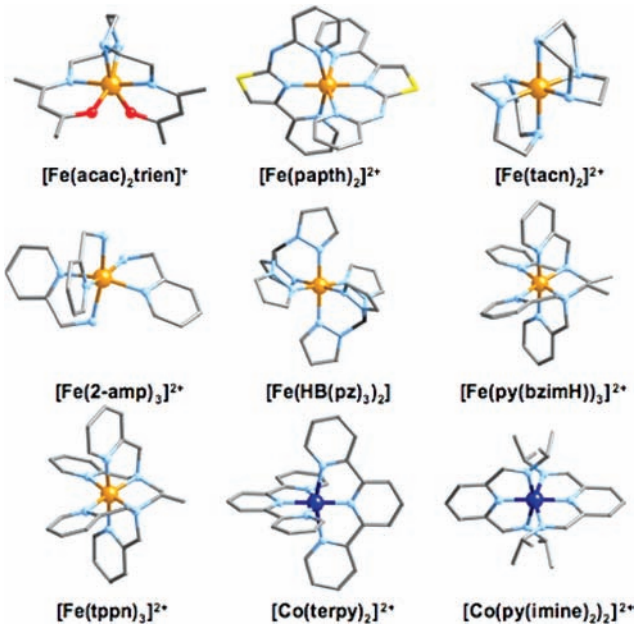

Figure 1. Crystal structures of complexes investigated in this study. Ligand abbreviations: acac = acetylacetonate, trien = triethylenetetramine, papth = 2-(2-pyridylamino)-4-(2-pyridyl)thiazole, tacn = 1,4,7-triazacyclononane, 2-amp = 2-aminomethylpyridine, $HP(pz)_3$ = hydrotris(pyrazol-1-yl)borate, py(bzimH) = 2-(2′-pyridyl)benzimidazole, tppn = tetrakis(2-pyridylmethyl)-1,2-propanediamine, terpy = terpyridine, $py(imine)_2$ = N-R-2,6-pyridinedicarboxaldimine.

study suggests that the hybrid meta functional TPSSh[6,26] with 10% exact exchange is optimal for modeling bond energies of a wide range of first-row transition metal systems.[19] For main-group molecular systems, TPSSh generally performs similar to B3LYP for the G3/99 set,[27] but its improved performance for transition metal systems[28] makes it particularly attractive.

An important chemical energy that has so far been an "enfant terrible" of computational chemistry is the energy difference between electronic configurations of different M_S quantum numbers, i.e., with different numbers of excess spin-up electrons.[12,18,21] It is anticipated on the basis of the recent findings[19] that TPSSh will outperform other functionals for modeling such spin-inversion energies. There is evidence that less than 20% exact exchange is needed to solve this problem, as seen, e.g., in a BP86 hybrid with 10% exact exchange[25] or in the modified B3LYP* with 15% exact exchange.[24,29−31]

There is substantial interest in accurately estimating spin inversion energies of first-row transition metals since spin inversion occurs in many important natural processes,[32,33] e.g., ligand binding to metalloproteins,[19] and since more accurate computations will pave the way for molecular design of spin-crossover systems for use in molecular magnetism, catalysis, and molecular storage,[34−36] all of which are problems that have been studied in detail by DFT.[24,31,37,38]

Other recent, related DFT studies of transition metal systems include studies of metal−metal bonds,[39] where nonhybrid TPSS performs well,[40] equilibrium geometries,[41] bond energies,[17,42] spin-inversion,[18−21,43−45] excitation energies,[46] as well as other data used to benchmark a large number of functionals.[12,42]

Here we report the study of nine spin-crossover complexes, seven with iron and two with cobalt (Figure 1), for which experimental enthalpies of spin crossover are available,[47] providing a direct quantitative test of functionals for this difficult task (see Table 1). This work compares the two most widely used functionals in inorganic chemistry, the hybrid 20%-exchange functional B3LYP and the GGA functional BP86, to the meta hybrid 10%-exchange functional TPSSh, the nonhybrid meta functional TPSS, and the meta functionals M06 and M06L.[48] It is found that TPSSh displays an unparalleled low MAE of ∼11 kJ/mol in spin crossover enthalpies. Since these energies directly reflect a balance of the exchange correlation in the systems, it implies that ∼10% exact exchange gives the most balanced description of exchange correlation in these first-row transition metal systems.

TABLE 1: Summary of Relevant Parameters for Test Molecules: Formula, Oxidation State of Metal, d-Electronic Configuration, ΔH^0 (kJ/mol) of Spin Crossover, and Reference Code in the Cambridge Structural Database

compound	M^{n+}	d^n	ΔH^0 (kJ/mol)	ref code
$[Fe(acac)_2trien]^+$	Fe^{3+}	d^5	7−17[49]	actrfe[50]
$[Fe(papth)_2]^{2+}$	Fe^{2+}	d^6	16[51]	coljao[52]
$[Fe(tacn)_2]^{2+}$	Fe^{2+}	d^6	21−24[53]	dettol[54]
$[Fe(2\text{-}amp)_3]^{2+}$	Fe^{2+}	d^6	18−25[55]	fepicc[56]
$[Fe(HB(pz)_3)_2]$	Fe^{2+}	d^6	16−22[57]	hpzbfe[58]
$[Fe(py(bzimH))_3]^{2+}$	Fe^{2+}	d^6	20−21[59]	kokfof[60]
$[Fe(tppn)]^{2+}$	Fe^{2+}	d^6	25−30[61]	zusdia[62]
$[Co(terpy)_2]^{2+}$	Co^{2+}	d^7	9−16[63]	casxid[64]
$[Co(py(imine)_2)_2]^{2+}$	Co^{2+}	d^7	11−17[65]	iqiceq[66]

Methods

The experimental enthalpies were obtained from single molecules in organic solvents with a variety of mainly spectroscopic and kinetic methods that estimate the enthalpy difference between the high-spin and low-spin states at standard conditions. Such observables do not contain effects of interactions within lattices, and intermolecular effects are expected to be quite small.[47] The key to using such data as quantitative benchmarks for density functionals in the same way as bond dissociation energies have been used[12] is to assume that the high- and low-spin states are in thermal equilibrium and thus can be geometry optimized as single molecules and their equilibrium energies and enthalpies computed.

All calculations were performed with the Turbomole 5.9 software.[67] Starting geometries were taken from the Cambridge Structural Database.[68] Electronic energies were converged down to 10^{-6} hartree, and to achieve stable equilibrium geometries, the gradient was converged down to 10^{-3} au. All electronic configurations with $M_S = 0, {}^1/_2, 1, {}^3/_2, 2, {}^5/_2$, or 3 were geometry optimized, depending on the oxidation state of the studied complex (e.g., 0, 1, and 2 for Fe^{II}) to yield stable energies on the potential energy surfaces.

Enthalpy corrections were calculated from subsequently computed harmonic frequencies for each configuration separately, by thermodynamic analysis. Zero-point energies are usually slightly smaller in the high-spin configurations, where bonds are weaker; however, the differences were in this case smaller than 7 kJ/mol and any scaling factor of 0.95−1.00 will affect the relative energies by less than 0.5 kJ/mol, which is expected since no bonds are broken. Thus, scaling factors have not been applied, and the numbers presented and discussed in this work are enthalpies at standard conditions (298 K, 1 atm), as are the experimental data.

The basis set used for geometry optimization was def2-SVP.[69] The larger 6-311+G(2d,2p) basis set was applied to test the influence of basis set size on the computed spin inversion energies. The energies of the high-spin and low-spin configurations of $[Co(terpy)_2]^{2+}$ and $[Fe(2\text{-}amp)_3]^{2+}$ were computed using both basis sets. The results shown in Figure 2

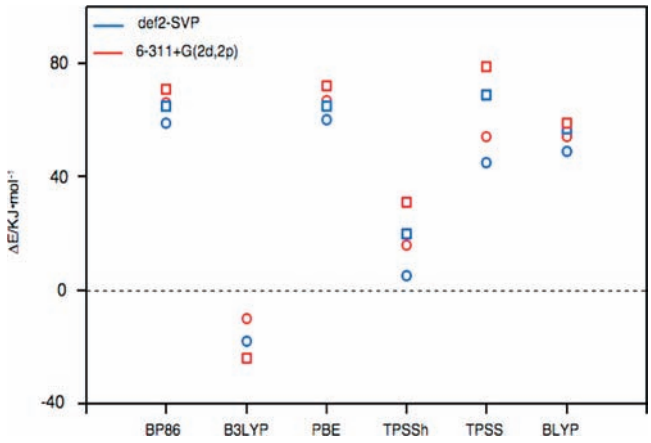

Figure 2. Effect of basis set on the energy difference between high- and low-spin configurations for $[Co(terpy)_2]^{2+}$ (empty circles) and $[Fe(2\text{-amp})_3]^{2+}$(empty squares). Blue is for the def2-SVP basis set, and red is for the larger 6-311+G(2d,2p) basis set.

show that the effect of the functional dominates by a factor of at least 5, whereas basis set effects are quite small for these types of energies, as compared to, e.g., ionization energies or electron affinities. For instance, ΔE predicted with BP86 for $[Co(terpy)_2]^{2+}$ is 55 kJ/mol, whereas B3LYP gives −18 kJ/mol. On the other hand, the larger basis set increases the energy difference by 2−11 kJ/mol for all the tested functionals, and the systematic component of this error may reduce the accuracy of the methods somewhat; however, the conclusion that TPSSh is the best performer is not affected by such an error. Because of these observations, the spin-crossover systems were described with the def2-SVP basis set. Numerical data can be found in Table S1 of Supporting Information.

Functionals BLYP and PBE were included to prove the point that all these GGA functionals (BP86, TPSS, BLYP, and PBE) provide similar results, with B3LYP farthest way and TPSSh in between; this confirms that the main determinant of these energies is indeed the amount of exact exchange included in the functional.For the six functionals studied in this work, the amount of exact exchange is zero for BP86, TPSS, and M06L, providing a nonhybrid version of each class of functional, whereas it is 10% for TPSSh, 20% for B3LYP, and 27% for M06.[48] Among the two schools of density functional development, the TPSS school emphasizes nonempirical functionals and rigorous approach, with TPSS being essentially nonempirical,[6,27] whereas the M06 school emphasizes pragmatic approach to highest accuracy, using some 30+ parameters.[48] Also for this reason, the two classes of functionals constitute an interesting comparison.

Results and Discussion

Computed Enthalpies of Spin Crossover. The computed differences in enthalpies of the configurations with different M_S corresponding to high-spin and low-spin are compared to experimental enthalpies[47] of spin crossover in Figure 3 (see Table 2 for numerical results).

As seen, BP86 and TPSS provide similar results as has also been observed for other types of chemical energies,[19] implying that the amount of exact exchange is more important than the inclusion of the kinetic energy density in modeling chemical processes. These nonhybrid functionals tend to overestimate, whereas B3LYP underestimates the enthalpies of spin crossover, since exact exchange directly favors the configurations with more aligned spins.

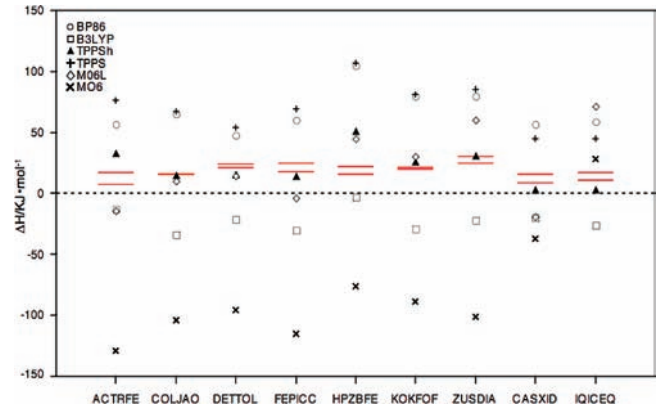

Figure 3. Computed and experimental enthalpies of spin crossover (kJ/mol).

TABLE 2: Experimental and Computed Enthalpies of Spin Crossover (kJ/mol)

model	ΔH_{exp}	BP86	B3LYP	TPSSh	TPSS	M06L	M06
$[Fe(acac)_2trien]^+$	7−17	57	−13	33	70	−14	−129
$[Fe(papth)_2]^{2+}$	16	65	−34	15	67	10	−104
$[Fe(tacn)_2]^{2+}$	21−24	48	−21	16	54	14	−96
$[Fe(2\text{-amp})_3]^{2+}$	18−25	60	−30	14	69	−4	−115
$[Fe(HB(pz)_3)_2]$	16−22	105	−3	51	107	45	−76
$[Fe(py(bzimH))_3]^{2+}$	20−21	80	−29	26	81	30	−89
$[Fe(tppn)]^{2+}$	25−30	80	−22	31	85	60	−101
$[Co(terpy)_2]^{2+}$	9−16	57	−20	3	45	−19	−37
$[Co(py(imine)_2)_2]^{2+}$	11−17	59	−26	3	45	71	28
MAE[a]		50	40	11	51	25	101
LAE[b]		86	52	32	88	33	137

[a] Calculated from experimental estimates, e.g., (17 + 7)/2 = 12 for $[Fe(acac)_2trien]^+$. [b] Largest absolute error.

The computed MAEs for the explored functionals are 50 kJ/mol (BP86), 40 kJ/mol (B3LYP), 11 kJ/mol (TPSSh), 51 kJ/mol (TPSS), 25 kJ/mol (M06L), and 101 kJ/mol (M06). Also in terms of largest absolute errors (LAE), TPSSh deviates the least from the experimental results: BP86 and TPSS display LAEs of 86 and 88 kJ/mol (for $[Fe(HB(pz)_3)]$); the LAE for B3LYP is 52 kJ/mol (for $[Fe(2\text{-amp})_3]^{2+}$). On the other hand, the LAE for TPSSh is 32 kJ/mol (for $[Fe(HB(pz)_3)]$). For the Minnesota functionals, the LAEs are 33 and 137 kJ/mol, respectively, for M06L and M06.

On the basis of these numbers, TPSSh is the functional that reproduces the experimental values the most accurately, with the meta density functional M06L a distant second. Considering that M06L has been constrained to be a "local" nonhybrid density functional, its performance is impressive, and it is a very promising entry point for future developments also within the inorganic chemistry community. Furthermore, by comparing TPSS and BP86 (similar results) against TPSSh (10% exact exchange) and B3LYP (20% exact exchange), the linear trend in computed energies as a function of exact exchange is very clear. Thus, the M06 functional, which contains the most exact exchange (27%), is the worst performer.

Importantly, the superiority of the TPSSh functional is reflected in both the iron and cobalt complexes, with the TPSSh-computed enthalpies of spin crossover for CASXID and IQICEQ close to 0 kJ/mol and within 10 kJ/mol of experimental values.

Whereas it has earlier been seen[19] that most chemical energies correlate linearly with the amount of exact exchange, it is hard to provide quantitative proof that 10% exact exchange is optimal for the d-block, as experimental data in thermal equilibrium are scarce. Benchmarks involving excitation energies to other

TABLE 3: Experimental Geometries of $[Fe(2\text{-amp})_3]^{2+}$ at $T = 12$ and 298 K, Compared with Geometries for Electronic Configurations Optimized with TPSSh

	12 K	298 K	$M_S = 0$	$M_S = {}^1/_2$	$M_S = 1$	$M_S = {}^3/_2$	$M_S = 2$	$M_S = {}^5/_2$
$Fe-N_1$	2.024	2.179	2.034	2.042	2.153	2.278	2.252	2.243
$Fe-N_2$	1.991	2.195	1.990	2.023	1.982	2.040	2.207	2.144
$Fe-N_3$	2.020	2.180	2.035	2.031	2.267	2.092	2.253	2.213
$Fe-N_4$	2.004	2.220	1.994	2.012	2.179	2.229	2.218	2.161
$Fe-N_5$	2.034	2.183	2.027	2.023	2.203	2.052	2.229	2.213
$Fe-N_6$	1.998	2.213	1.989	2.016	1.983	2.010	2.208	2.160
MAE 12 K			0.009	0.016	0.124	0.105	0.216	0.177
MAE 298 K			0.184	0.171	0.103	0.114	0.035	0.048

electronic configurations will have issues of, e.g., geometry optimizing the correct equilibrium geometries. Thus, the experimental enthalpies of thermal conversion between high- and low-spin isomers of cobalt and iron complexes in our opinion provide an ideal and strict test of density functionals in the same way that metal−ligand bond dissociation energies do.

Errors in spin-inversion energies and bond dissociation energies are diagnostic of the imbalance of exchange and correlation in molecular systems. An ideal theoretical method must describe in a balanced way electron correlation in all states of both of these, and other, processes. The present results show (i) that experimental spin-crossover enthalpies can be described accurately by DFT-computed electronic spin inversion energies using vibration analysis and thermodynamic corrections; (ii) that the functional TPSSh provides an unprecedented good description of such experimental enthalpies; (iii) that this success is *mainly* due to the 10% exact exchange of the functional. These conclusions are fully consistent with the conclusions obtained from metal−ligand bond dissociation energies and imply that 10% exact exchange provides the optimal balance of correlation effects for chemical processes involving first-row transition metal systems.

Geometries of Spin-Crossover Complexes. Although the main purpose of this work is to evaluate the accuracy of functionals for computing spin inversion energies, relevant information resides in the various equilibrium structures obtained from geometry optimizing individual electronic configurations. Importantly, whereas the geometry of an excited state is generally not experimentally accessible, the equilibrium geometries of spin-crossover complexes at temperatures below and above the transition temperature are expected to represent the respective low-spin and high-spin electronic states of the complexes.

As an example of the usefulness of this observation, the six Fe−N bond lengths of the equilibrium structure of $[Fe(2\text{-amp})_3]^{2+}$ computed with TPSSh are shown in Table 3. For this complex, crystallographic structures are available at both high (298 K) and low (12 K) temperature for comparison with the six possible "candidate" electronic configurations with $M_S = 0$, ${}^1/_2$, 1, ${}^3/_2$, 2, and ${}^5/_2$. Ferric states were included to test for the possibility of achieving false positives. Geometric data for the remaining structures are found in Table S2 of Supporting Information.

Looking at Table 3, the Fe−N bond lengths differ substantially in the two sets of crystal data, with the structure at low T having on average 0.18 Å shorter Fe−N bond lengths. This corresponds well to the change in state from low-spin with all electrons occupying "bonding" d orbitals pointing away from the ligands, to high-spin with electrons occupying "anti-bonding" d-orbitals directed toward the N ligands.

As seen in Table 3, the geometries of the six optimized electronic configurations illustrate this well. In fact, the correct ferrous ground states with $M_S = 0$ and $M_S = 2$ can be deduced directly from the two computed structures in best agreement with experimental data at 12 and 298 K, respectively. It is known that geometries can be reproduced quite accurately with DFT,[12,28,42] giving typical metal−ligand bond lengths in error by less than ∼0.05 Å. Thus, DFT computations are accurate enough to identify electronic states from distinct experimental structures of the same molecule, which is particularly encouraging. The Fe−N bond lengths for the Fe^{II} low-spin state are predicted to within 0.009 Å and those for the Fe^{II} high-spin state are predicted to within 0.035 Å on average. Other electronic configurations are ruled out on this basis, although the ferric high-spin state ($M_S = {}^5/_2$) is very similar in structure to the ferrous high-spin state ($M_S = 2$). It is important to notice that if so-called intermediate spin states ($M_S = 1$ for Fe^{II} and 3/2 Fe^{III}) or quantum admixed states (e.g., $M_S = 1,2$ for Fe^{II}) can occur the assignment is sometimes no longer unambiguous, as Table S2 in Supporting Information illustrates in the case of $[Fe(acac)_2trien]^+$.

Figure 4 shows the overlap of crystal structures at low and high temperature with TPSSh-optimized low- and high-spin configurations, respectively, showing the very good agreement between computed and experimental structures, even considering the significant changes occurring upon spin crossover.

The performance of the functionals BP86 and B3LYP for describing the structures of the two electronic states ($M_S = 0$ and $M_S = 2$) has been evaluated in Table 4. It can be seen that B3LYP, which performed poorly in terms of estimating enthalpies of spin crossover, also overestimates the metal−ligand bond legths in all cases, giving a MAE of the six bond lengths 0.041 and 0.060 Å for the low-spin and high-spin states, respectively. The tendency of exact exchange to increase metal−ligand bond lengths is well established[12,17,19,28,40,42] and correlates with the tendency of polarizing electrons.[12,19] This leads correspondingly to underestimation of bond strengths and bias toward more distributed electrons (in terms of quantum numbers), e.g., higher

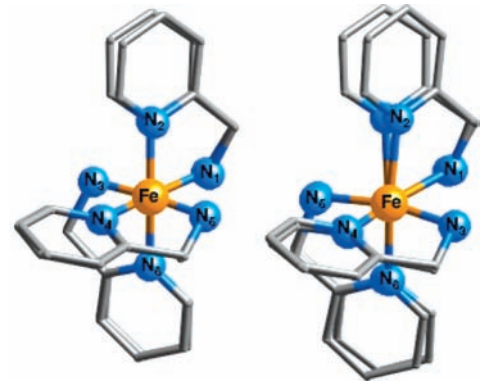

Figure 4. Overlap of experimental and TPSSh-computed structures for high-spin and low-spin $[Fe(2\text{-amp})_3]^{2+}$.

TABLE 4: Experimental Geometries of $[Fe(2\text{-amp})_3]^{2+}$ at $T = 12$ and 298 K, Compared with Low- and High-Spin Geometries for TPSSh, BP86, and B3LYP

	$T = 12$ K, Low-spin ($M_S = 0$)				$T = 298$ K, High-spin ($M_S = 2$)			
	Crystal	TPSSh	BP86	B3LYP	Crystal	TPSSh	BP86	B3LYP
$Fe-N_1$	2.024	2.034	2.032	2.071	2.179	2.252	2.254	2.266
$Fe-N_2$	1.991	1.990	1.982	1.982	2.195	2.207	2.202	2.250
$Fe-N_3$	2.020	2.035	2.036	2.073	2.180	2.253	2.251	2.269
$Fe-N_4$	2.004	1.994	1.986	2.058	2.220	2.218	2.221	2.251
$Fe-N_5$	2.034	2.027	2.022	2.067	2.183	2.229	2.234	2.250
$Fe-N_6$	1.998	1.989	1.984	2.047	2.213	2.208	2.203	2.246
MAE		0.009	0.013	0.041		0.035	0.036	0.060

spin and angular quantum numbers, and effectively larger occupation of "anti-bonding" orbitals.[12,19]

The BP86 functional gives significantly better geometries, as seen for more general and large test sets of transition metal compounds.[12] The MAEs are reduced substantially to 0.013 and 0.036 Å for the low-spin and high-spin states, respectively. As seen in Table 4, BP86 has a small tendency to underestimate bond lengths of the low-spin state, usually reflected also in too large computed bond strengths.[12,19] Thus, in terms of structure, BP86 reproduces experimental geometries almost as well as TPSSh (MAEs of 0.009 and 0.035 Å) but still performs significantly worse for computing the associated energies of the electronic states. However, BP86 will also in general (with exception of intermediate spin cases, as mentioned above) predict the electronic state solely from the experimental structures.

Figure 5 displays the geometric results obtained with TPSSh for the iron complexes, for which low-spin and high-spin structures are not available. On the basis of the accuracy deduced from the discussion of $[Fe(2\text{-amp})_3]^{2+}$ above, we can directly infer the electronic state that must correspond to each experimental structure. As seen in Figure 5, in each case, one electronic state is significantly closer to experimental data, allowing for such an assignment. This shows that DFT, in the form of TPSSh, not only accurately predicts the enthalpy of spin crossover to ~11 kJ/mol but also predicts the electronic states of iron coordination compounds solely from the experimental structures, by comparing the theoretical alternatives.

In all other cases, we can predict the electronic state representative of the experimental crystal structure with statistical confidence from the MAEs of computed metal−ligand bond lengths. Thus, the experimental crystal structures correspond to the following electronic states: $[Fe(acac)_2trien]^+$ is ferric high-spin, $M_S = {}^5/_2$; $[Fe(papth)_2]^{2+}$ is ferrous high-spin, $M_S = 2$; $[Fe(tacn)_2]^{2+}$ is low-spin, $M_S = 0$; $[Fe(2\text{-amp})_3]^{2+}$ is high-spin, $M_S = 2$; $[Fe(HB(pz)_3)_2]$ is low-spin, $M_S = 0$; $[Fe(py(bzimH))_3]^{2+}$ is high-spin, $M_S = 2$; $[Fe(tppn)]^{2+}$ is low-spin, $M_S = 0$.

In the case of cobalt complexes, the structural effects upon spin crossover are less pronounced, and thus it is harder to predict the electronic state based solely on experimental structural data. This is because only one electron changes orbital on going from the $M_S = {}^1/_2$ to $M_S = {}^3/_2$ state, implying occupation of one antibonding d-orbital. Thus, the predictive power of TPSSh for deducing the electronic state from the structure is stronger in the case of iron complexes, simply due to the larger real structural effects upon spin crossover.

However, as we saw earlier, the subtle energy differences between electronic configurations, and thus the enthalpy of spin crossover, are predicted equally well with TPSSh in the case of cobalt complexes.

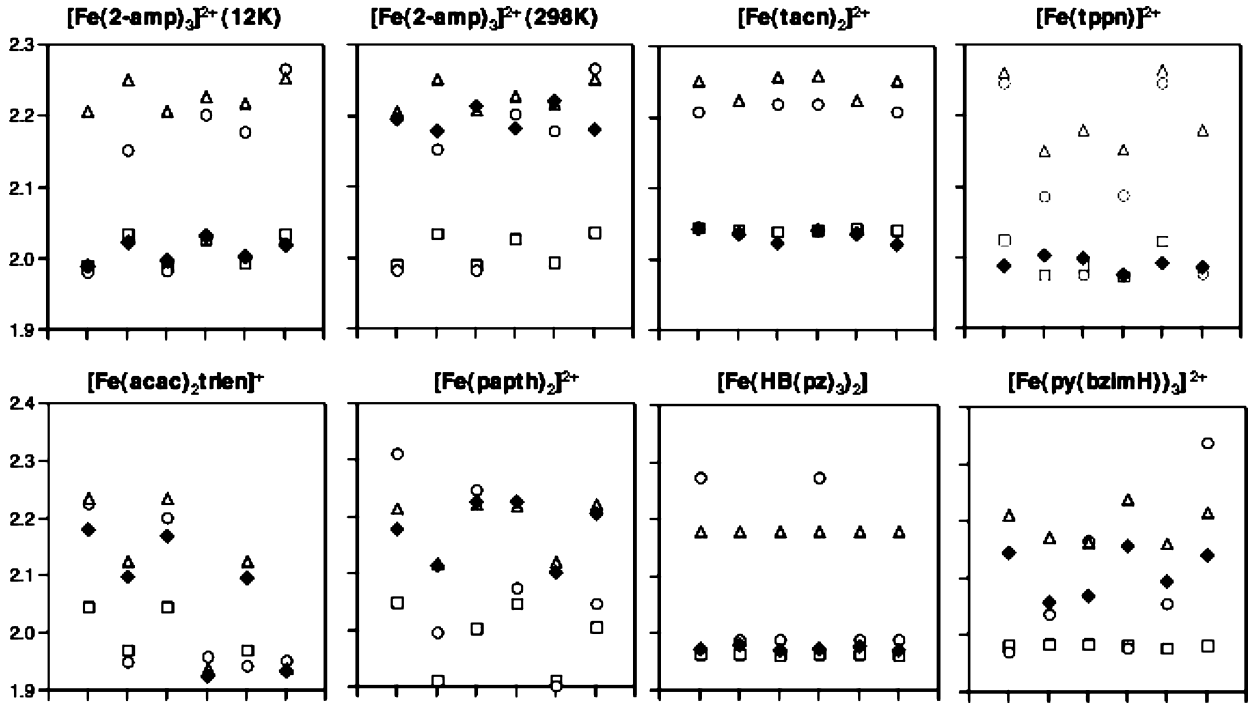

Figure 5. Equilibrium bond lengths of iron complexes for crystal structures (black rhombs) and TPSSh-computed electronic configurations with $M_S = 0$ (white squares), 1 (white circles), and 2 (white triangles), respectively ($M_S = {}^1/_2$, ${}^3/_2$, and ${}^5/_2$ for $[Fe(acac)_2trien]^+$).

Conclusions

Many investigations into spin crossover, molecular magnetism, close-lying electronic states, etc., are routinely performed by computational chemists, although errors in the chemical energies can exceed 100 kJ/mol.[12,19] This casts doubt on many previous conclusions drawn from such studies. In processes where the electronic structure changes qualitatively, a good theoretical method must treat electron correlation in a consistent and balanced manner on both sides of the reaction equation. Since Fermi correlation is the major cause of differential correlation energy in such cases, the treatment of exchange in density functionals is a key to obtaining accurate and consistent chemical energies.

In the d-block, many important valence electronic configurations have similar energies, implying large nondynamical correlation and a need to balance Fermi correlation when electron pairs are separated. In fact, less than 20% exact exchange as found in B3LYP can be argued on grounds of perturbation theory to be optimal in first-row transition metal systems.[23]

This paper has reported computations of enthalpies for nine spin-crossover complexes with six functionals, viz., the widespread BP86 (nonhybrid GGA) and B3LYP (hybrid, 20% exact exchange) functionals as well as the more modern meta functionals TPSS (nonhybrid), TPSSh (hybrid, 10% exact exchange), M06L (nonhybrid), and M06 (hybrid, 27% exact exchange).

It has been shown that the 10%-exact exchange meta hybrid functional TPSSh as the first of *any theoretical method* reaches an accuracy close to 10 kJ/mol (11 kJ/mol for our data set) for enthalpies of spin crossover and by interpolation, for providing a balanced description of Fermi correlation, as also witnessed in studies of metal−ligand bond dissociation energies.[19] This is true for both iron and cobalt complexes. The M06L functional provides surprisingly good energies as well, with a mean absolute error of 25 kJ/mol. All other functionals display mean absolute errors in excess of 40 kJ/mol, the reasons being clearly identifiable as due to too much or too little exact exchange. There may be some systematic errors in the procedure, in particular related to basis set effects, which could be as large as ∼10 kJ/mol. Such effects will however not change the conclusion that TPSSh provides the most balanced treatment of the involved electronic states, as judged from the agreement with experimental enthalpies.

Furthermore, we demonstrate the predictive value of DFT (emphasized by TPSSh) for deducing the electronic state of a coordination complex based on its experimental structure. This prediction requires computation of the geometries of all possible candidate electronic states using this functional.

The main result of this work, together with earlier work,[19] is the confirmation that TPSSh is so far the most accurate functional we have tested for computing chemical energies (bond breaking, ion ionization energies, ligand binding, and spin inversion) of molecules involving d-block metals. The most important physical reason is that 10%-exact exchange provides a proper balance between Fermi correlation effects on both sides of the reaction equation, whereas more exact exchange (as in, e.g., B3LYP) overemphasizes the atomic, dissociated, and spin aligned states, whereas less exact exchange (as in nonhybrid functionals such as BP86 and TPSS) emphasizes the molecular, bound, and spin-coupled state.

The benchmarks used to develop the M06 series of functionals involved some transition metal data[48] and for metal−ligand binding energies, TPSSh and M06, and M06L performed similar, whereas for other energies, TPSSh performed worse; this is surprising given the clear evidence that important chemical processes involving transition metals are linear in the amount of exact exchange. Given the present and earlier[19] results, it is suggested that a Minnesota functional including 10% exact exchange is explored.

The accuracy of TPSSh for these processes is not likely to be surpassed by any ab initio method in the near future, and we therefore recommend to use this particular functional in studies of first-row transition metal systems until a more accurate and equally fast theoretical method has been developed. Even more appealing is then the fact that this functional is largely nonempirical, left the exact exchange parameter;[27] the M06 functionals contain some 30+ parameters.[48]

Acknowledgment. K.P.J. acknowledges support from the Danish Natural Science Research Council (Steno Fellowship, Grant No. 272-08-0041) and The Danish Center for Scientific Computing. J.C. gratefully acknowledges support from the Generalitat de Catalunya (Beatriu de Pinos Fellowship, 2006 BP-A 10041).

Supporting Information Available: Tables containing numbers for accessing the basis set effects and all metal−ligand bond lengths of TPSSh-optimized spin-crossover complexes compared with crystal data. This material is available free of charge via the Internet at http://pubs.acs.org.

References and Notes

(1) Kohn, W.; Becke, A. D.; Parr, R. G. *J. Phys. Chem.* **1996**, *100*, 12974–12980.
(2) Parr, R. G.; Yang, W. *Density Functional Theory of Atoms and Molecules*; Oxford University Press: New York, 1989.
(3) Ziegler, T. *Chem. Rev.* **1991**, *91*, 651–667.
(4) Siegbahn, P. E. M. *J. Biol. Inorg. Chem.* **2006**, *11*, 695–701.
(5) Geerlings, P.; De Proft, F.; Langenaeker, W. *Chem. Rev.* **2003**, *103*, 1793–1873.
(6) Tao, J.; Perdew, J. P.; Staroverov, V. N.; Scuseria, G. E. *Phys. Rev. Lett.* **2003**, *91*, 146401.
(7) Becke, A. D. *J. Chem. Phys.* **1993**, *98*, 5648–5652.
(8) Zhao, Y.; Truhlar, D. G. *Acc. Chem. Res.* **2008**, *41*, 157–167.
(9) Bausclicher, C. W. *Chem. Phys. Lett.* **1996**, *246*, 40–44.
(10) Siegbahn, P. E. M.; Blomberg, M. R. A. *Chem. Rev.* **2000**, *100*, 421–437.
(11) Harvey, J. N. *Annu. Rep. Prog. Chem. Sect. C* **2006**, *102*, 203–226.
(12) Jensen, K. P.; Roos, B. O.; Ryde, U. *J. Chem. Phys.* **2007**, *126*, 014103.
(13) Langhoff, S. R.; Bauschlicher, C. W., Jr. *Annu. Rev. Phys. Chem.* **1988**, *39*, 181–212.
(14) Frenking, G.; Frohlich, N. *Chem. Rev.* **2000**, *100*, 717–774.
(15) Becke, A. D. *Phys. Rev. A* **1988**, *38*, 3098–3100.
(16) Perdew, J. P. *Phys. Rev. B* **1986**, *33*, 8822–8824.
(17) Jensen, K. P.; Ryde, U. *J. Phys. Chem. A* **2003**, *107*, 7539–7545.
(18) Neese, F. *J. Biol. Inorg. Chem.* **2006**, *11*, 702–711.
(19) Jensen, K. P. *Inorg. Chem.* **2008**, *47*, 10357–10365.
(20) Zein, S.; Borshch, S. A.; Fleurat-Lessard, P.; Casida, M. E.; Chermette, H. *J. Chem. Phys.* **2007**, *126*, 014105.
(21) Daku, L. M. L.; vargas, A.; hauser, A.; Fouqueau, A.; Casida, M. E. *ChemPysChem* **2005**, *6*, 1393–1410.
(22) Harris, J.; Jones, R. O. *J. Phys. F* **1974**, *4*, 1170–1186.
(23) Perdew, J. P.; Ernzerhof, M.; Burke, K. *J. Chem. Phys.* **1996**, *105*, 9982–9985.
(24) Reiher, M. *Inorg. Chem.* **2002**, *41*, 6928–6935.
(25) Schenk, G.; Pau, M. Y. M.; Solomon, E. I. *J. Am. Chem. Soc.* **2004**, *126*, 505–515.
(26) Perdew, J. P.; Tao, J.; Staroverov, V. N.; Scuseria, G. E. *J. Chem. Phys.* **2004**, *120*, 6898–6911.
(27) Staroverov, V. N.; Scuseria, G. E.; Tao, J.; Perdew, J. P. *J. Chem. Phys.* **2003**, *119*, 12129–12137.
(28) Furche, F.; Perdew, J. P. *J. Chem. Phys.* **2006**, *124*, 044103.
(29) Conradie, J.; Ghosh, A. *J. Phys. Chem. B* **2007**, *111*, 12621–12624.
(30) Brewer, G.; Olida, M. J.; Schmiedekamp, A. M.; Viragh, C.; Zavalij, P. Y. *Dalton Trans.* **2006**, 5617–5629.

(31) Paulsen, H.; Trautwein, A. X. *Top. Curr. Chem.* **2004**, *235*, 197–219.
(32) Real, J. A.; Gaspar, A. B.; Munoz, M. C. *Dalton Trans.* **2005**, *12*, 2062–2079.
(33) Goodwin, H. A. *Coord. Chem. Rev.* **1976**, *18*, 293–325.
(34) König, E.; Madeja, K. *Inorg. Chem.* **1967**, *7*, 1848–1855.
(35) Gutlich, P.; Hauser, A.; Spiering, H. *Angew. Chem., Int. Ed. Engl.* **1994**, *33*, 2024–2054.
(36) Postnikov, A. V.; Bihlmayer, G.; Blugel, S. *Comput. Mater. Sci.* **2006**, *36*, 91–95.
(37) Hauser, A.; Enachescu, C.; Daku, M. L.; Vargas, A.; Amstutz, N. *Coord. Chem. Rev.* **2006**, *250*, 1642–1652.
(38) Zhang, Y.; Oldfield, E. *J. Phys. Chem. A* **2003**, *107*, 4147–4150.
(39) Barden, C. J.; Rienstra-Kiracofe, J. C.; Schaefer, H. F., III. *J. Chem. Phys.* **2000**, *113*, 690–700.
(40) Zhao, Y.; Truhlar, D. G. *J. Chem. Phys.* **2006**, *124*, 224105.
(41) Buhl, M.; Kabrede, H. *J. Chem. Theory Comput.* **2006**, *2*, 1282–1290.
(42) Schultz, N. E.; Zhao, Y.; Truhlar, D. G. *J. Phys. Chem.* **2005**, *109*, 11127–11143.
(43) Respondek, I.; Bressel, L.; Saalfrank, P.; Kampf, H.; Grohmann, A. *Chem. Phys.* **2008**, *347*, 514–522.
(44) Swart, M.; Groenhof, A. R.; Ehlers, A. W.; Lammertsma, K. *J. Phys. Chem. A* **2004**, *108*, 5479–5483.
(45) Sorkin, A.; Iron, M. A.; Truhlar, D. G. *J. Chem. Theory Comput.* **2008**, *4*, 307–315.
(46) Holthausen, M. C. *J. Comput. Chem.* **2005**, *26*, 1505–1518.
(47) Turner, J. W.; Schultz, F. A. *Coord. Chem. Rev.* **2001**, *219*−*221*, 81–97.
(48) Zhao, Y.; Truhlar, D. G. *Theor. Chem. Acc.* **2008**, *120*, 215–241.
(49) Dose, E. V.; Murphy, K. M. M.; Wilson, L. J. *Inorg. Chem.* **1976**, *15*, 2622–2630.
(50) Sinn, E.; Sim, G.; Dose, E. V.; Tweedle, M. F.; Wilson, L. J. *J. Am. Chem. Soc.* **1978**, *100*, 3375–3390.
(51) Beattie, J. K.; Binstead, R. A.; West, R. J. *J. Am. Chem. Soc.* **1978**, *100*, 3044–3050.
(52) Baker, A. T.; Goodwin, H. A.; Rae, A. D. *Aust. J. Chem.* **1984**, *37*, 443–447.
(53) Turner, J. W.; Schultz, F. A. *Inorg. Chem.* **1999**, *38*, 358–364.
(54) Boeyens, J. C. A.; Forbes, A. G. S.; Hancock, R. D.; Wieghardt, K. *Inorg. Chem.* **1985**, *24*, 2926–2931.
(55) Chum, H. L.; Vanin, J. A.; Holanda, M. I. D. *Inorg. Chem.* **1982**, *21*, 1146–1152.
(56) Chernyshov, D.; Hostettler, M.; Tornroos, K. W.; Burgi, H.-B. *Angew. Chem., Int. Ed.* **2003**, *42*, 3825–3830.
(57) Jesson, J. P.; Swiatoslaw, T.; Eaton, D. R. *J. Am. Chem. Soc.* **1967**, *89*, 3158–3164.
(58) Oliver, J. D.; Mullica, D. F.; Hutchinson, B. B.; Milligan, W. O. *Inorg. Chem.* **1980**, *19*, 165–169.
(59) Reeder, K. A.; Dose, E. V.; Wilson, L. J. *Inorg. Chem.* **1978**, *17*, 1071–1075.
(60) Peng, S. M.; Chen, H.-F. *Bull. Inst. Chem. Acad. Sin.* **1990**, *37*, 49–64.
(61) McGarvey, J. J.; Lawthers, I.; Heremans, K.; Toftlund, H. *Inorg. Chem.* **1990**, *29*, 252–256.
(62) McCusker, J. K.; Rheingold, A. L.; Hendrickson, D. N. *Inorg. Chem.* **1996**, *35*, 2100–2112.
(63) Beattie, J. K.; Binstead, R. A.; Kelso, M. T.; Del Favero, P.; Dewey, T. G.; Turner, D. H. *Inorg. Chim. Acta* **1995**, *235*, 245–251.
(64) Figgis, B. N.; Kucharski, E. S.; White, A. H. *Aust. J. Chem.* **1983**, *36*, 1527–1535.
(65) Simmons, M. G.; Wilson, L. J. *Inorg. Chem.* **1977**, *16*, 126–130.
(66) Juhasz, G.; Hayami, S.; Inoue, K.; Maeda, Y. *Chem. Lett.* **2003**, *32*, 882–883.
(67) Ahlrichs, R.; Bär, M.; Häser, M.; Horn, H.; Kölmel, C. *Chem. Phys. Lett.* **1989**, *162*, 165–169.
(68) Allen, F. H. *Acta Crystallogr.* **2002**, *B58*, 380–388.
(69) Weigend, F.; Ahlrichs, R. *Phys. Chem. Chem. Phys.* **2005**, *7*, 3297–3305.

JP900654J